Research Article | Vol. 11, No. 1 / 1 January 2021 / Optical Materials Express 157
Optical Materials EXPRESS

# GLS-Se optical fibre from extruded glass structured preforms and rods for the IR region

FERNANDO GUZMAN,[1,*] CHRISTOPHER CRAIG,[1] BRUNO MOOG,[1] ANDREA RAVAGLI,[2] AND DANIEL W. HEWAK[1]

[1] Optoelectronics Research Centre, Southampton, SO17 1BJ, UK
[2] Schott AG, Hattenbergstraße 10, 55122, Mainz, Germany
[*] f.a.guzman-cruz@soton.ac.uk

**Abstract:** Depending on composition, chalcogenide glasses have been proven as a reliable medium to transmit light in the range from the visible to the long-wave infrared (LWIR), specialty glasses based on gallium lanthanum sulfide (GLS) with a selenium (Se) addition. This family of glasses offers a broad transparency window depending on the composition. Their optical, mechanical, and thermal properties have been exploited in their bulk form. In this paper, we demonstrate the fabrication of optical fibres from extruded structured (core-clad) preforms and rods, with an emphasis on maintaining the intrinsic characteristics of the glass and exploiting the optical fibre geometry for light delivery.



## 1. Introduction

One method to obtain optical fibre from chalcogenide glasses includes using previously manufactured glass rods and structured (core-clad) solid preforms produced by extrusion, as this technique has been proven reliable for this type of glasses in the past [1]. The principle behind drawing this family of glasses into an optical fibre follows the same technique as any other known glass [2,3]. A glass rod is set into a furnace, temperature is raised above the softening point and then the glass is drawn into a suitable optical fibre diameter [4] depending on the application, the geometry and dimensions might vary. Initial thoughts indicated that this process was straightforward as the thermal properties of GLS-Se based glasses have been studied previously [5], and theoretical results have been pictured, making this family of glasses suitable for fibre drawing. Fibre drawing from solid preforms favours glasses based on GLS compared to crucible drawing [6], as these family of glasses have melting temperatures on the order of 1000 °C, which is higher compared to other conventional chalcogenide glasses which have a melting point in the range of 300–500 °C [7].

In the past other chalcogenide glasses have been drawn into optical fibres, with different results [8]. An advantage of this type of glasses over silica-based glasses, is their feasibility to be drawn into fibres at relatively low temperatures [9], making the process itself simpler and more flexible. The main challenge for chalcogenide glass preforms is the tendency to crystallize [10], as their softening point is close to the crystallization temperature requiring to reduce the time consumed in the process to avoid promoting nucleation [11] while the glass rod is being heated. Also, the viscosity curve is steep [12], so variations in temperature need to be avoided to have a successful process outcome.

Previous work [13] has considered chalcogenide glasses with some oxygen content [14], where rods and preforms are directly produced from bulk samples [15] and with no imperfections within the glasses. These aspects have helped in the obtaining of reliable GLS based optical fibres [16]. As seen in the previous studies GLS-Se glasses have been produced and analysed [17] but this is

#411571 https://doi.org/10.1364/OME.411571
Journal © 2021 Received 5 Oct 2020; revised 5 Dec 2020; accepted 7 Dec 2020; published 16 Dec 2020

Optical Materials EXPRESS

the first time that is shown that this family of glasses can be exploited from rod and structured preforms and subsequently drawn into fibre.

## 2. Method

For silica fibres, preforms which provide the internal core-clad structure of the resulting fibre are manufactured by chemical vapour deposition (CVD) [18] which provides a glass that is highly stable and can be heated to its softening temperature without subsequent nucleation or crystal growth, resulting in low loss optical fibres [19]. No equivalent CVD process has been developed for preform fabrication from chalcogenide glasses. Therefore, as an alternative method for shaping the bulk chalcogenide glass into a preform, or rod, to then fabricate optical fibre extrusion has been explored [20]. Bulk GLS-Se glass samples with 20 mol%, 30 mol% and 35 mol% of $Ga_2Se_3$ were fabricated following previous studies methodology [21], where the glass samples are produced by melt-quenching of the raw materials at 1150 °C in cylindrical carbon crucibles, with a diameter of 30 mm, and a thickness of 30–35 mm, which then are annealed at 490 °C and finally moulded into rods by extrusion using a maximum temperature of 610 °C for all compositions, a temperature above the transition temperature ($T_g$) while avoiding the crystallization temperature ($T_x$) for at least 182 °C. Extrusion was carried at a rate of 0.5 mm/min.

### 2.1. Rod and structured preform preparation for fibre drawing

The extruded structured glass preforms (core-clad), and rods, must undergo some preparation steps before they are suitable for fibre drawing. Each extrusion produces between 15 to 26 cm of extruded glass depending on the volume of the glass billet (Fig. 1). The fibre drawing tower furnace configurations has been optimized for rods of around 10 cm in length which is optimum to be able to maintain control over the samples. This means that each glass rod to be drawn needs to be cut down to a suitable length (Fig. 2), and notches are made in both ends to be able to hold the extruded rod inside the furnace and to add extra weight to promote the necking of the rod to start the fibre drawing process.

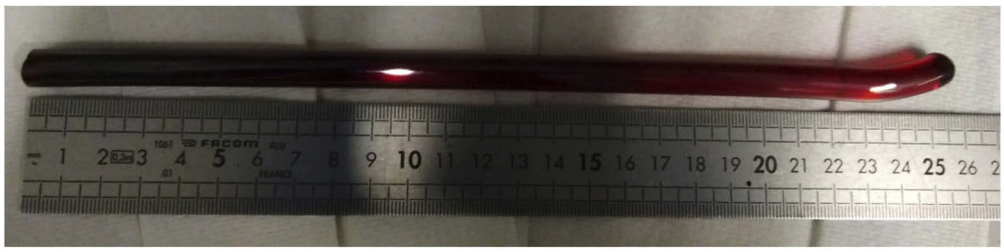


**Fig. 1.** Extruded structured preform based on GLS-Se glasses.

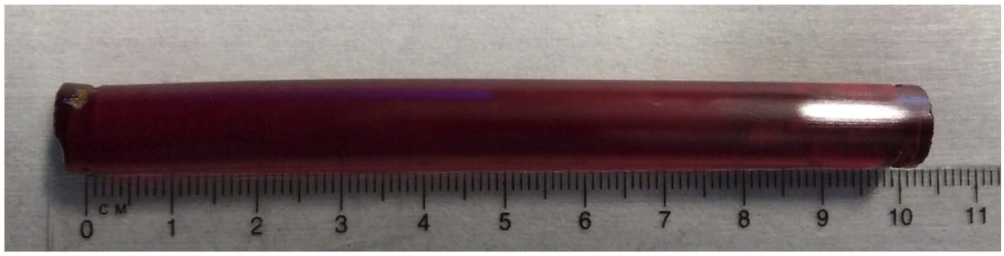


**Fig. 2.** Cut extruded glass rod (10 cm) suitable to fit the fibre drawing furnace.

Optical Materials EXPRESS

The first fibre drawing attempts did not consider the surface quality of the extruded rods and structured preforms. Initial experiments only considered the post-extrusion crystallization on the surface to be detrimental for fibre drawing. Some of the extruded preforms, and rods, came out of the die scratched or contaminated, which led to further thoughts about how to overcome these surface imperfections. First thoughts were to repeat the experiments and not use said extruded rods, as some higher quality, extruded rods were obtained with no apparent surface imperfections and except for the strays produced by the friction between the die and the glass flowing outwards (Fig. 3). The strays have a width of 10 µm and a separation of 7 µm between them. These good quality extruded rods were obtained by reducing the extrusion temperature from 630 °C to 610 °C. Some of these transparent rods with no surface crystals could not be drawn, as they showed heavy crystallization and weak fibre after drawing. These results demonstrated that apart from the use of the correct temperature, the surface quality of the extrusion had some influence, as it is known that poor surface quality promotes crystallization, as the microscopical strays can act as the volume needed to act as a nucleus [22].

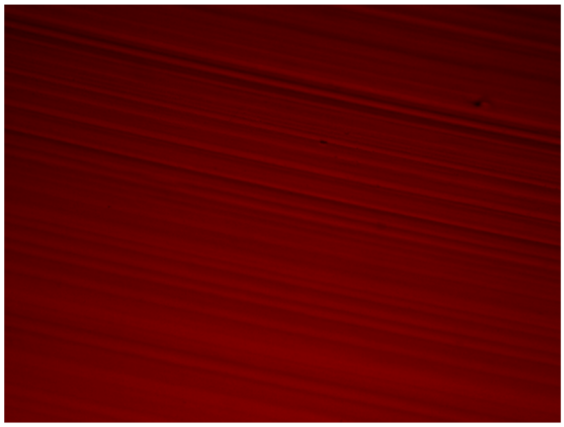

**Fig. 3.** Surface strays produced by friction during the extrusion.

### 2.2. Rod and structured preform surface polishing

To overcome any imperfection and produce a smooth surface to facilitate fibre drawing, each extruded rod was polished down to 1 µm of grit size. For this, a small in-house constructed lathe (Fig. 4 and 5) and Thorlabs diamond films were used. This added step modified completely the surface (Figs. 6 and 7) and enhanced the outcome of fibre drawing. One disadvantage is that this step was not automated [23] and was done entirely by hand, so a lot of expertise needs to be obtained by practice before being able to produce reliable rod polishing for fibre drawing (Fig. 8).

After the polishing is finished a cleaning step is performed, with the ultrasonic bath and isopropanol to remove any residual ethanediol, used for polishing, left on the surface. The cleaned rod, or structured preform, is attached to the silica holder and a weight of 80 g is place in the other end, helping to maintain the rod in a straight position and to aim the necking in the fibre drawing process (Figs. 9 and 10).

### 2.3. Fibre drawing

The next step is to place the preform holder, extruded polished rod (or structured preform) and weight vertically in the fibre drawing tower RF furnace (Fig. 10). This step is crucial as they must be positioned without touching any element of the furnace, as they can be misplaced affecting with this the process. The rod needs to be positioned exactly in the middle of the furnace, were

Optical Materials EXPRESS

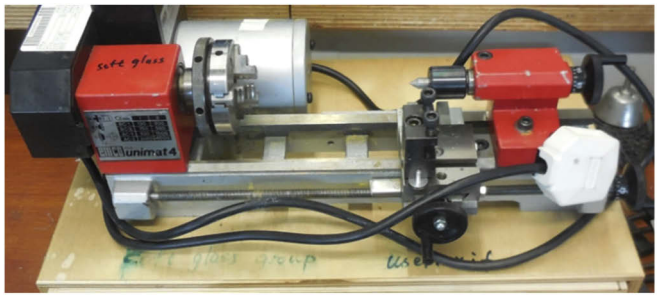


**Fig. 4.** Lathe for rod polishing.

**Fig. 5.** Extruded rod during polishing.

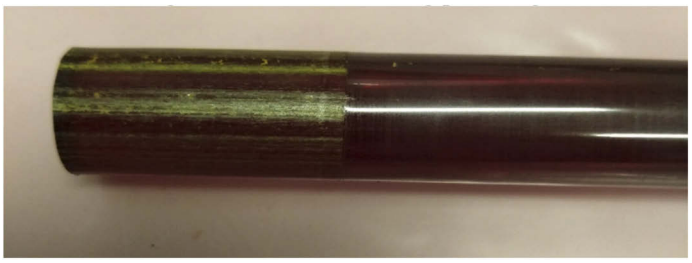

**Fig. 6.** Surface scratched rod, showing the benefits of polishing.

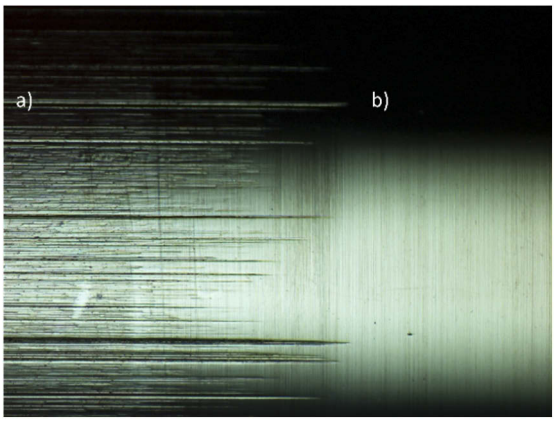


**Fig. 7.** Extruded rod a) unpolished and b) polished surfaces down to 1 µm of grit size.

Optical Materials EXPRESS

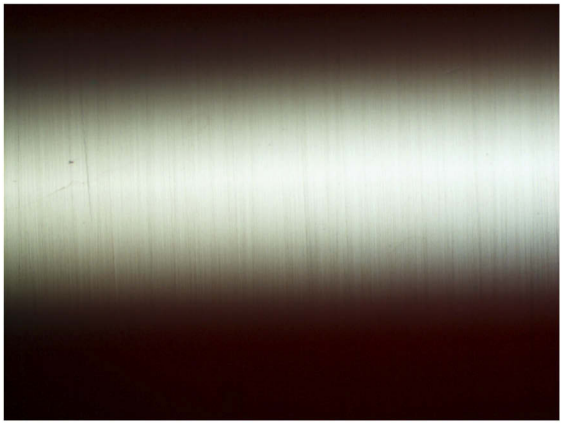

**Fig. 8.** Completely polished extruded rod surface.


**Fig. 9.** Examples of extruded and polished rods where a) is attached to the silica holder and the 80 g weight, and b) has a length of 11 cm and is ready to be set on the furnace. Surface quality is clearly seen.

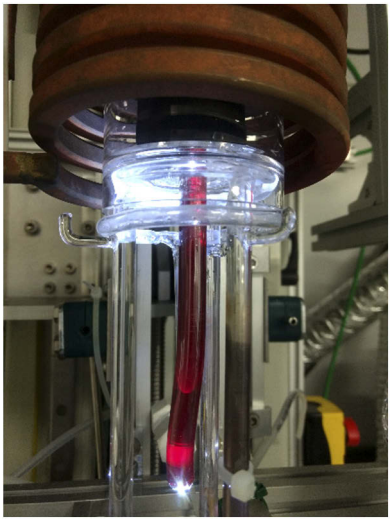

**Fig. 10.** Structured extruded and polished preform, set in the middle of the furnace before fibre drawing.

Optical Materials EXPRESS

the centre of the rod is concentric to the centre of the furnace, as this assures an even surface and volume heating of the rod [24]. Any misaligning means that part of the rod gets hotter and this produces a viscosity mismatch; this surface thermal difference is also translated as a need to supply more heat to soften the less hot glass region, incrementing the chance of crystallization.

### 2.4. *Thermal studies to understand the behaviour of the GLS-Se glasses during fibre drawing*

To understand whether the steps were correctly executed and to discard any possible non-dependent variables, Differential Thermal Analysis (DTA) and Thermomechanical Analysis (TMA) were carried for extruded GLS-Se samples for which the quality was already proved to be the best at that time. These studies comprise using different heating ramping rates to provide a better understanding of the thermal and mechanical behaviour of the glass and check if these parameters remain consistent or if there was a different behaviour as a function of the heating rate.

For the DTA samples of 30 mg from the bulk of the unpolished extruded structured preform were used. As seen in Fig. 11, if the heating rate is increased the crystallization peak is displaced to the right, this variation is due to the nature of the activation energy of the glass [25]. This is of importance as it shows that the position of the crystallization peak relies fundamentally upon the heating rate, as the glass relaxes isothermally towards a new enthalpy equilibrium that is temperature dependant [26]. For the heating rate of 20 °C/min there is a slight inconsistency in the trend as this sample had a bigger mass compared to the others that remained constant. Table 1 enlists the $T_g$ and $T_x$ of the extruded GLS-Se preform at different heat rates. The span between temperatures goes from $T_x$ - $T_g$ = 168 to 174, this demonstrates the thermal stability of the glasses [27] and confirms the ability to be drawn into fibres.

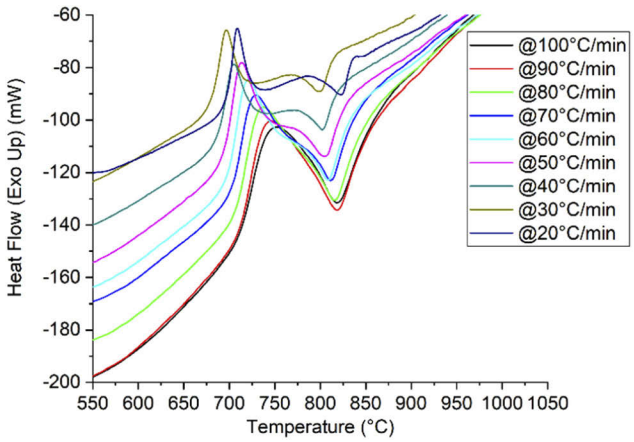


**Fig. 11.** DTA for an extruded structured GLS-Se preform at different heating rates.

Another aspect to consider in the fibre drawing process is the viscosity, as it is temperature dependant. To understand if there is a change in viscosity related to the ramping rate of the fibre drawing furnace (100 °C/min), a TMA was performed with different heating rates. As seen in Fig. 12, (a) slow heat rate is preferred as it ensures all the volume of the glass is heated uniformly compared to a higher heat rate where the viscosity curve is steeper. This results in a situation where the surface of the glass presents a temperature difference compared to the inside [28], producing with this an undesired effect where the surface is ready to be drawn while the inside remains at a higher viscosity. The viscosity curve also needs to be related with the time the glass is exposed to temperature inside the furnace, as a high viscosity enables longer exposure without crystallization, but is probable fibre would not be easily obtained. On the other hand, a low

Optical Materials EXPRESS

**Table 1. Transition and crystallization temperatures of an extruded GLS-Se preform at different heating rates**

| Heating Rate (°C/min) | $T_g$ (°C) | $T_x$ (°C) |
|---|---|---|
| 20 | 537 | 695 |
| 30 | 511 | 679 |
| 40 | 514 | 686 |
| 50 | 515 | 691 |
| 60 | 521 | 697 |
| 70 | 527 | 701 |
| 80 | 529 | 707 |
| 90 | 534 | 709 |
| 100 | 536 | 710 |

viscosity could dramatically reduce the time of exposure needed to draw a fibre, but maybe even little exposure would lead to crystallization. To explore the time of exposure for GLS-Se glasses a time-temperature-transformation (TTT) needs to be carried in future studies.

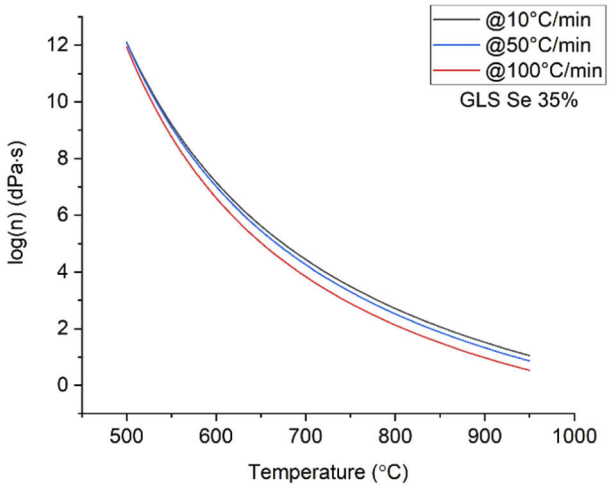


**Fig. 12.** TMA for an extruded glass rod at different heat rates.

These thermal and mechanical studies in extruded glass had the objective to simulate the behaviour of the glass in the drawing tower. The value of this information is more theoretical as the skills to obtain reliable optical fibre remain practical, but these extra studies helped understand that the ramping rate can be used in favour of avoiding crystallization in the same way as using lower temperatures, as the viscosity and crystallization peak values are displaced.

## 3. Results

Thermal and mechanical studies in conjunction with previous fibre drawing attempts demonstrated that each composition requires specific parameters (i.e. temperature) and expertise. The biggest challenge with this family of chalcogenide glasses is that there is no previous literature that could explain in depth the behaviour of the glass when they are thermally treated during processing (i.e. optical fibre drawing). One of the problems encountered is that once the temperature is adequate, and set in the furnace, the process needs to go as fast as possible to avoid crystallization

Optical Materials EXPRESS

while working with a viscosity suitable for optical fibre to be obtained. Therefore, there must be a compromise between the temperature, and feed and drum speeds while controlling the tension of the fibre. This means that high tensions can be used if viscosity is in a value low enough to avoid mechanical stresses that could break the glass rod or fibre, during the optical fibre diameter control. After considering all these aspects, it is good to finally point out that the fibre drawing process does not occur in the actual hot zone (forming region), but it occurs in the already heated and viscous glass (draw-down region) [29], at this point the cooling rate for the fibre becomes essential to avoid crystals and breakage from thermal shock (Fig. 13 and 14). All rods and structured preforms were polished before fibre drawing. Temperatures for the rods were set higher compared to the temperatures used for structured preforms as the approach was to decrease the viscosity and obtain fibres as fast as possible. For the structured preforms lower temperatures were set at the expense of having a higher viscosity and longer fibre drawing time. Both approaches were carried trying to avoid crystallization during the process.

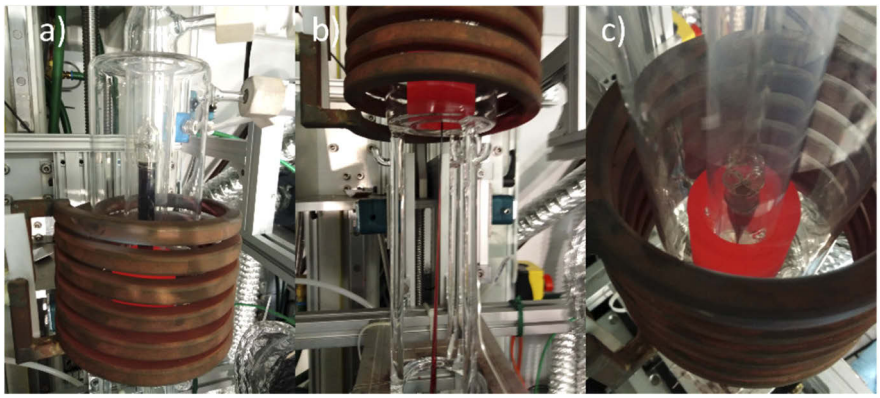


**Fig. 13.** Fibre drawing process for GLS-Se glass rods and structured preforms where a) is the rod inside the furnace being heated, b) is the beginning of the fibre obtention, and c) the neck profile is clearly seen inside the furnace.

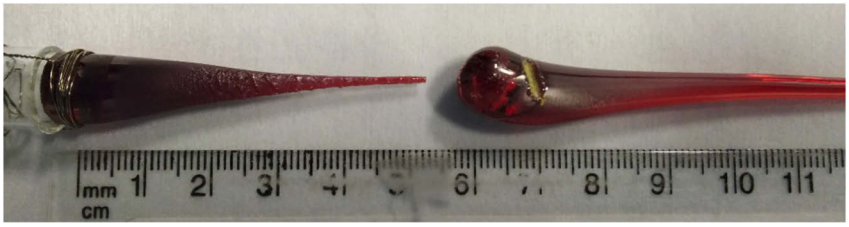


**Fig. 14.** First and last part of the extruded rod after fibre drawing, where the neck presents some surface crystallization due to the time consumed in the whole process.

### *3.1. GLS-Se optical fibre drawing from glass rods of a single composition*

Before being able to draw structured preforms, the goal was to obtain optical fibre from single rod compositions, to verify the steps required and to address any challenge that might arise from the complexity of the process itself. Three compositions of GLS-Se with 20 mol%, 30 mol% and 35 mol% of $Ga_2Se_3$ were produced in extruded rods and these were drawn into fibre. Temperatures between 780 °C and 800 °C, feed speeds between 0.5 and 2 mm/min, and drum speeds between 2 to 5 m/min were used during the processes. Optical fibre with diameters between 200 μm and

Optical Materials EXPRESS

250 µm, and lengths up to 50 m were obtained (Fig. 15). To measure the losses and characterize the fibre (Figs. 16–18) the cut back method was used along with an optical spectrum analyser (OSA) and an ARCoptix portable FTIR, for the range of 600 nm to 1.7 µm, and 2 to 5 µm respectively, showing minimum losses around 10 dB/m in some compositions at 4µm. Losses vary through compositions, and further research must be carried to determine if the fibre drawing process increases the losses or if the raw materials have a direct relation with them, however, it is demonstrated that extruded GLS-Se glass rods can be drawn into optical fibre.

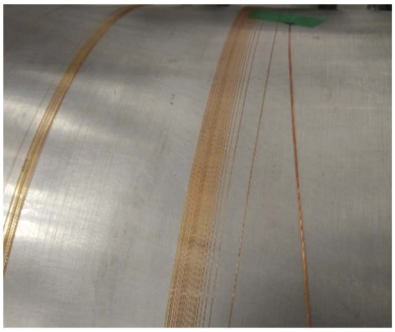

**Fig. 15.** GLS-Se optical fibre collected in the drum after the fibre drawing process.

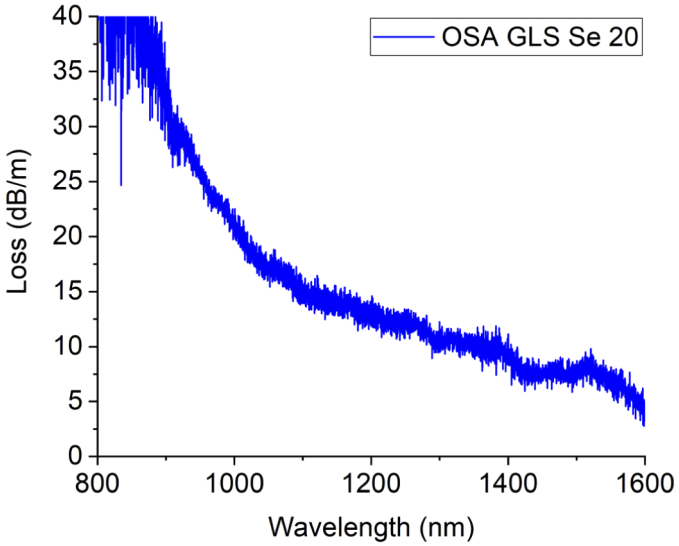


**Fig. 16.** GLS-Se with $Ga_2Se_3$ 20 mol% optical fibre losses (800 nm−1.6 µm).

### *3.2. GLS-Se optical fibre from structured preforms*

Structured preforms were fabricated using GLS-Se glasses with $Ga_2Se_3$ concentrations of 35 mol% and 30 mol%, for the core and cladding respectively, as they present refractive indexes of 2.42 and 2.40 respectively [30] and a NA of 0.31. As these compositions are thermally and mechanically similar [31] the decision was made to establish a middle ground and use a maximum drawing temperature of 710 °C and a minimum of 690 °C. These are the lowest temperatures ever used, and the approach taken was to wait until the neck was produced and then to start

Optical Materials EXPRESS

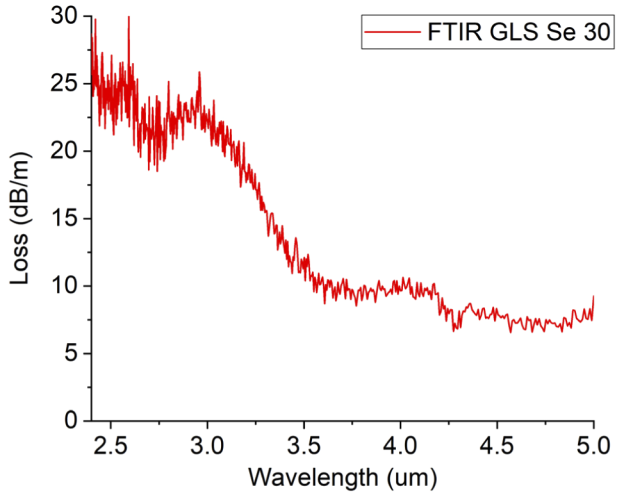


**Fig. 17.** GLS-Se with $Ga_2Se_3$ 30 mol% optical fibre losses (2.4–5 µm).

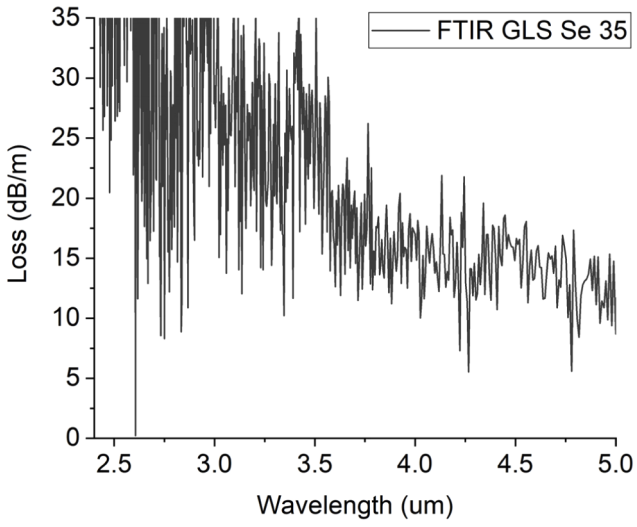


**Fig. 18.** GLS-Se with $Ga_2Se_3$ 35 mol% optical fibre losses (2.4–5 µm). Signal-to-noise ratio varies as this can be an effect of non-homogeneity of the fibre over long lengths after the fibre drawing process (i.e. difference and amount of crystals at different sections).

Optical Materials EXPRESS

decreasing the temperature by 2 °C until the fibre was attached to the drum. Temperature was only decreased, and drum speed modified to adjust tension and diameter. Being meticulous paid off as the success rate for fibre drawing was of 100%, this means that from when the fibre was attached to the drum for collection the process was never stopped, and no breakage was produced at any moment until the glass was finished. For the first time continuous and uninterrupted long lengths (up to 220 m) of GLS-Se optical fibre were produced, with the best surface quality to date (Figs. 19, 20 and 21).

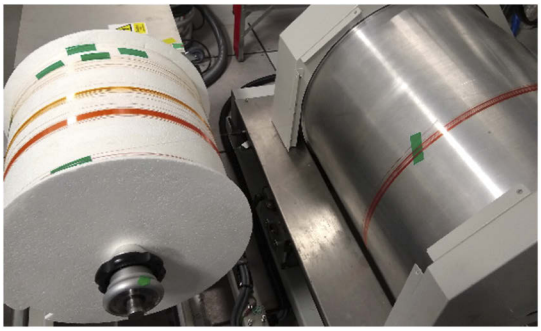

**Fig. 19.** GLS-Se structured optical fibre being transferred from the drum to a bobbin.

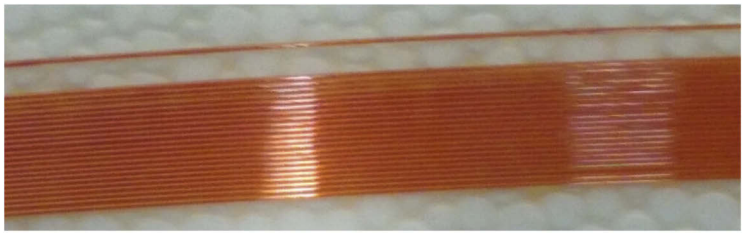

**Fig. 20.** Close up of GLS-Se structured optical fibre.

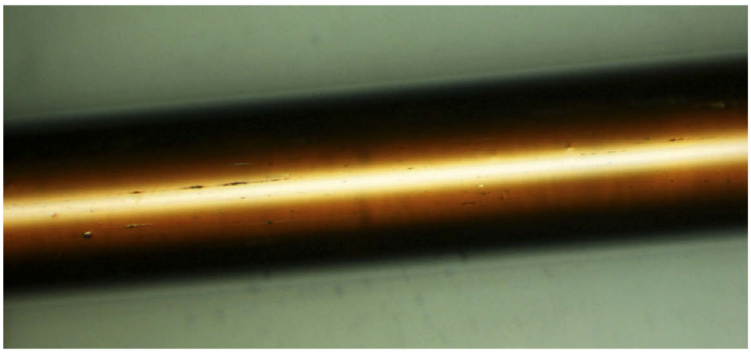

**Fig. 21.** GLS-Se optical fibre of 210 µm in diameter, with the lowest surface defects ever achieved.

One future goal to achieve is the control in the core diameter size for GLS-Se structured optical preforms, by the use of a two-die assembly [32]. Therefore, the same applies for GLS-Se structured optical fibre where the core diameter varies depending the section of the preform that

Optical Materials EXPRESS

is drawn into a fibre (Figs. 22). Same as with single composition glass rods, the obtained fibre diameters are between 190–250 μm. These proof of principle results can lead to the obtention of thinner fibre and to achieve smaller diameters. This can establish a possibility of decreasing the losses in the fibre [33]. Characterization of the fibres used the cutback method and an ARCoptix portable FTIR, for clarity only the lowest values obtained are shown (Fig. 23).

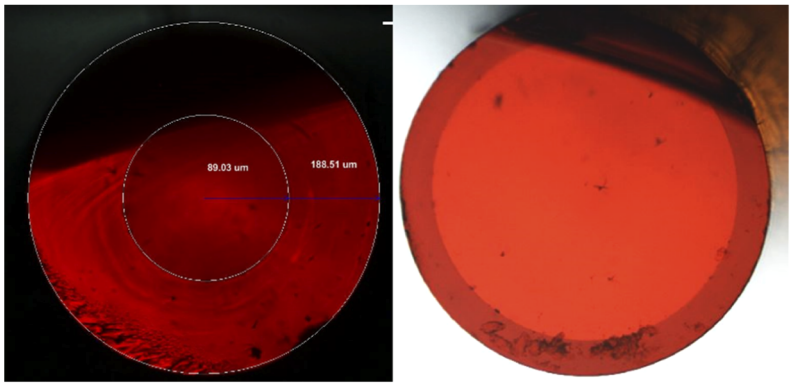


**Fig. 22.** Structured GLS-Se optical fibre showing different core diameters

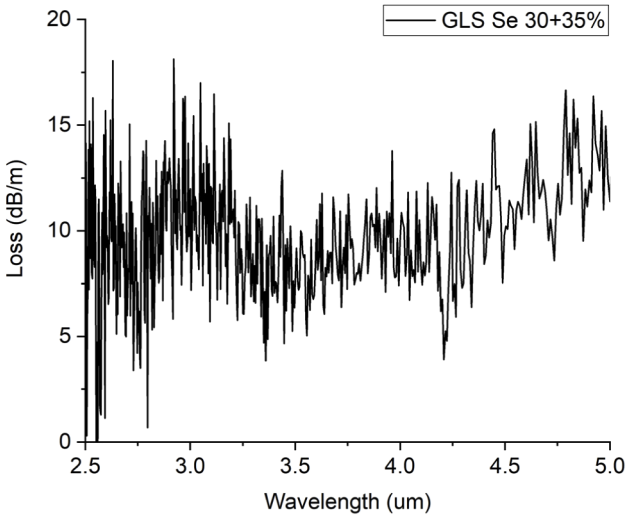


**Fig. 23.** Structured GLS-Se optical fibre losses

## 4. Conclusion

GLS-Se glass rods and structured preforms have been drawn into optical fibres for the first time with losses of 10–15 dB/m. This achievement required a solid practical expertise of the thermal and mechanical characteristics of these chalcogenide glasses. The main challenge to draw GLS-Se glasses into an optical fibre is to maintain their original bulk properties, as additional thermal processing could modify their structure and processing steps might add contaminant particles. However, the results shown in this work prove that GLS-Se optical fibres are now an option to continue exploring applications in the optics industry, such as high-power fibre lasers,

Optical Materials EXPRESS

IR light confinement, and leaves space for improving the transmission at longer wavelengths to exploit in full the properties of GLS-Se glasses as optical fibres.

## Funding

Engineering and Physical Sciences Research Council (EP/M015130/1); Consejo Nacional de Ciencia y Tecnología (739108).

## Acknowledgements

To the Optoelectronic Research Centre (ORC) for the facilities, each member of the Novel Glass Group lead by Prof. Dan W. Hewak for some ideas and training, Ed Weatherby for technical support, Nick White for assistance with extrusion and Paul Frampton for glass blowing.

This work was sponsored in part by CONACYT-Mexico and the Faculty of Physical Sciences and Engineering, Southampton. Chalcogenide glass research at Southampton is also supported through the Engineering and Physical Sciences Research Council (EPSRC) through research grant EP/M015130/1, Manufacturing and Application of Next Generation Chalcogenides.

## Disclosures

The authors declare no conflicts of interest.

## References

1. R. R. Gattass, D. Rhonehouse, D. Gibson, C. C. McClain, R. Thapa, V. Q. Nguyen, S. S. Bayya, R. J. Weiblen, C. R. Menyuk, L. B. Shaw, and J. S. Sanghera, "Infrared glass-based negative-curvature anti-resonant fibers fabricated through extrusion," Opt. Express **24**(22), 25697–25703 (2016).
2. R. E. Jaeger, "Fiber drawing process: characterization and control," in *Fiber Optics: Advance in Research and Development*, B. Bendow and S. S. Mitra, eds. (Springer, 1979).
3. X. Zhang, H. Ma, and J. Lucas, "Applications of chalcogenide glass bulks and fibres," J. Optoelectron. Adv. Mater. **5**(12), 873–883 (2002).
4. J. Le Person, F. Smektala, T. Chartier, L. Brilland, T. Jouan, J. Troles, and D. Bosc, "Light guidance in new chalcogenide holey fibres from GeGaSbS glass," Mater. Res. Bull. **41**(7), 1303–1309 (2006).
5. A. Ravagli, *Development of Visible-to-LWIR Multispectral Chalcogenide Glasses* (University of Southampton, 2018).
6. W. H. Kim, V. Q. Nguyen, L. B. Shaw, L. E. Busse, C. Florea, D. J. Gibson, R. R. Gattass, S. S. Bayya, F. H. Kung, G. D. Chin, R. E. Miklos, I. D. Aggarwal, and J. S. Sanghera, "Recent progress in chalcogenide fiber technology at NRL," J. Non-Cryst. Solids **431**, 8–15 (2016).
7. R. Mossadegh, J. S. Sanghera, D. Schaafsma, B. J. Cole, V. Q. Nguyen, R. E. Miklos, and I. D. Aggarwal, "Fabrication of single-mode chalcogenide optical fiber," J. Lightwave Technol. **16**(2), 214–217 (1998).
8. D. Lezal, "Chalcogenide glasses-survey and progress," J. of Optoelectron. and Adv. Mater. **5**(1), 23–34 (2003).
9. D. W. Hewak, A. K. Mairaj, N. M. Petrovich, and Y. D. West, "Application of novel glass for the next generation of optical fibre devices," presented at Photonics 2000, Calcutta, India, 01 Dec. 2000.
10. J. W. Mullin, *Crystallization* (Butterworths, 1961).
11. R. Hand, R. Kangley, J. Shephard, D. Furniss, and A. Seddon, "GaLaS optical fibers: thermo-optical properties and fiber drawing," *Proc. SPIE* 4215, (2001).
12. N. G. R. Broderick, D. W. Hewak, T. M. Monro, D. J. Richardson, and Y. D. West, "Holey optical fibres of non-silica based glass," US 7,155,099 B2, (2006).
13. J. Sanghera, L. Shaw, and I. Aggarwal, "Rare earth doped infrared-transmitting glass fibers," in *Rare-Earth-Doped Fiber Lasers and Amplifiers*, M. J. F. Digonnet, ed. (CRC Press, 2001).
14. R. J. Curry, A. K. Mairaj, C. C. Huang, R. W. Eason, D. W. Hewak, and J. V. Badding, "Chalcogenide glass thin films and planar waveguides," J. Am. Ceram. Soc. **88**(9), 2451–2455 (2005).
15. T. Schweizer, D. J. Brady, and D. W. Hewak, "Fabrication and spectroscopy of erbium doped gallium lanthanum sulphide glass fibres for mid-infrared laser applications," Opt. Express **1**(4), 102–107 (1997).
16. D. W. Hewak, R. C. Moore, T. Schweizer, J. Wang, B. Samson, W. S. Brocklesby, D. N. Payne, and E. J. Tarbox, "Gallium lanthanum sulphide optical fibre for active and passive applications," Electron. Lett. **32**(4), 384 (1996).
17. A. Ravagli, C. Craig, G. A. Alzaidy, P. Bastock, and D. W. Hewak, "Optical, thermal, and mechanical characterization of $Ga_2Se_3$-added GLS glass," Adv. Mater. **29**(27), 1606329 (2017).
18. J. E. Townsend, S. B. Poole, and D. N. Payne, "Solution-doping technique for fabrication of rare-earth-doped optical fibres," Electron. Lett. **23**(7), 329–331 (1987).
19. T. Li, *Optical Fiber Communications: Fiber Fabrication* (Elsevier, 2012).

Optical Materials EXPRESS


20. A. B. Seddon, D. Furniss, and D. J. Sims, "Gallium-lanthanum-sulphide glasses: extrusion of fiber optic preforms and relevant physical properties," *Proc. SPIE* 3849 (1999).
21. A. Ravagli, C. Craig, J. Lincoln, and D. W. Hewak, "Ga-La-S-Se glass for visible and thermal imaging," Adv. Opt. Technol. **6**(2), 131–136 (2017).
22. R. Müller, E. D. Zanotto, and V. M. Fokin, "Surface crystallization of silicate glasses: nucleation sites and kinetics," J. Non-Cryst. Solids **274**(1-3), 208–231 (2000).
23. G. W. Fynn and W. J. A. Powell, *Cutting and Polishing Optical and Electronic Materials* (CRC Press, 1988).
24. G. K. Chui and R. Gardon, "Interaction of Radiation and Conduction in Glass," J. Am. Ceram. Soc. **52**(10), 548–553 (1969).
25. H. E. Kissinger, "Variation of Peak Temperature With Heating Rate in Differential Thermal Analysis," J. Res. Natl. Bur. Stan. **57**(4), 217–221 (1956).
26. O. A. Lafi, M. M. A. Imran, and M. K. Abdullah, "Glass transition activation energy, glass-forming ability and thermal stability of $Se_{90}In_{10-x}Sn_x$ (x=2, 4, 6 and 8) chalcogenide glasses," Phys. B **395**(1-2), 69–75 (2007).
27. G. Abbady and A. M. Abd-Elnaiem, "Thermal stability and crystallization kinetics of $Ge_{13}In_8Se_{79}$ chalcogenide glass," Phase Transitions **92**(7), 667–682 (2019).
28. X. Cheng and Y. Jaluria, "Optimization of a thermal manufacturing process: Drawing of optical fibers," Int. J. Heat Mass Transfer **48**(17), 3560–3573 (2005).
29. X. Cheng and Y. Jaluria, "Effect of furnace thermal configuration on optical fiber heating and drawing," Numer. Heat Transfer, Part A **48**(6), 507–528 (2005).
30. D. W. Hewak, A. Ravagli, and J. Lincoln, "Next generation chalcogenide glasses for visible and IR imaging," presented at SPIE Security + Defence and Remote Sensing 2016, Edinburgh, UK, 28 Sept. 2016.
31. A. Ravagli, C. Craig, K. A. Morgan, I. Zeimpekis, A. Aghajani, E. C. Weatherby, and D. W. Hewak, "Structural modification of Ga-La-S glass for a new family of chalcogenides," Proc. SPIE **10181**, 101810R (2017).
32. E. T. Y. Lee and E. R. M. Taylor, "Two-die assembly for the extrusion of glasses with dissimilar thermal properties for fibre optic preforms," J. Mater. Process. Technol. **184**(1-3), 325–329 (2007).
33. G. R. Newns, P. Pantelis, J. L. Wilson, R. W. J. Uffen, and R. Worthington, "Absorption losses in glasses and glass fibre waveguides," Opt. Quantum Electron. **5**(4), 289–296 (1973).